Crystalline potential for photoelectron scattering phase-shift calculations and X-ray absorption spectra of Ti in crystals

1991 J. Phys.: Condens. Matter 3 8967

(http://iopscience.iop.org/0953-8984/3/45/018)

J. Phys.: Condens. Matter 3 (1991) 8967–8979. Printed in the UK

Crystalline potential for photoelectron scattering phase-shift calculations and x-ray absorption spectra of Ti in crystals

L A Bugaev†, R V Vedrinskii†, I G Levin† and V M Airapetian‡

† Institute of Physics, Rostov State University, Stachka Avenue 194, Rostov-on-Don, 344104, USSR

‡ Yerevan Physics Institute, 2 Alykchanian Brothers Street, Yerevan, 375036, USSR

Received 19 April 1991

Abstract. X-ray absorption spectra (XAS) of Ti in crystals of Ti metal, TiC, TiN and TiO_2 rutile are calculated in EXAFS and XANES regions. Single, double and triple photoelectron scattering processes are included through the spherical-wave formalism and the crystalline muffin-tin (MT) potential model, which employs a Hartree–Fock exchange interaction between photoelectron and core electrons inside MT spheres. Overall agreement of the theoretical and experimental spectra is obtained on the absolute photon energy scale. This result enables one to treat the experimental XAFS without using adjustable parameter E_0. The neutral-atoms approximation is shown to be adequate for the phase-shift calculations in XAS theory for both metals and insulators. A comparison of Ti K XAFS of Ti metal calculated by means of various exchange–correlation potentials for the photoelectrons inside MT spheres is carried out. The best results are shown to be provided by Hartree–Fock and Dirac–Hara exchange potentials.

1. Introduction

The crystalline potential generation problem in the theory of x-ray absorption fine structure (XAFS) has been studied extensively in many papers [1]. Within a rigorous theoretical approach one should employ in this theory a non-local, complex, energy-dependent operator $\Sigma(r, r', \varepsilon)$ known as the Dyson self-energy [1]. This operator is self-consistent and consequently it cannot be described exactly as a superposition of the potentials of free atoms. Therefore any XAFS theory based on environment-independent uniform atomic potentials is *a priori* approximate. However, such an approximation, which provides transferable scattering phase shifts and amplitudes, is necessary if one intends to obtain structural information from XAFS. Hence, the goal of XAFS theory is to work out an approximate but reasonable model of the crystalline potential based on the muffin-tin (MT) approximation and transferable atomic potentials inside MT spheres. The main problems of potential generation in XAFS theory are the following: (i) the choice of MT sphere radii (R_{MT}) and exchange–correlation potentials inside MT spheres; (ii) the determination of the electron configurations of the atoms in the initial and final stages of the photoionization process; and (iii) the choice of the interstitial local constant potential named MT zero (ε_{MT}).

0953-8984/91/458967 + 13 $03.50

Different versions of the local electron density approximation inside MT spheres are employed in a great number of publications [1]. Lee and Beni [2] arrive at the conclusion that the traditional $X\alpha$ potential is inappropriate for extended x-ray absorption fine-structure (EXAFS) analysis and introduced a complex Hedin–Lundqvist (HL) exchange–correlation potential in EXAFS theory. Numerical results show that the photoelectron inelastic losses are taken into account by this potential in reasonable agreement with experiment [3–5]. However, the fine structures calculated with the help of HL potentials are often characterized by a contraction on the energy scale of the theoretical spectra compared to the experimental ones. Therefore, in [3, 6] the real Dirac–Hara (DH) exchange potential was used for the phase-shift and amplitude calculations, whereas the inelastic losses were introduced with the help of the imaginary part of the HL potential. In order to achieve good agreement with experiment, energy-dependent values of ε_{MT} and adjustable parameter E_0 obtained from the best agreement of the theoretical and experimental spectra were employed as well [5].

In [7] an alternative model for the crystalline potential was proposed based on the non-local energy-independent Hartree–Fock (HF) potential inside MT spheres and energy-independent value of ε_{MT}. The photoelectron inelastic losses were introduced phenomenologically through the traditional exponential factors [1]. Within this model theoretical XAFS of the molecules Br_2 and $GeCl_4$, the crystals Cu, Fe and Ge [8, 9] and alkali halides [10, 11] were obtained in good agreement with experiment. Calculated scattering phase shifts and amplitudes gave the opportunity to achieve high accuracy in the first-shell structure determinations by EXAFS [8]. In [12] the model proposed was improved by introducing new rules for choice of R_{MT} and ε_{MT} so as to provide crystalline potential continuity at MT sphere surfaces. As a result we obtained not only XAFS of the molecules and complexes containing low-Z atoms in reasonable agreement with experiment, but also good agreement of the calculated and experimental spectra on the photon energy (E_{ph}) scale [12]. In order to compare the spectra on the E_{ph} scale we combined the theoretical crystalline vacuum levels (VL) with VL positions of the experimental spectra. We consider the good agreement of the experimental and theoretical spectra on the E_{ph} scale to be the most sensitive criterion of the adequacy of the crystalline potential model.

In this paper the model proposed in [12] is applied to describe K XAFS of transition-series atoms in crystals. For this purpose Ti K XAFS of crystals of Ti, TiC, TiN and TiO_2 rutile are chosen because, first, up to now an adequate theoretical description of these spectra is absent and, secondly, the change of physical properties along the treated series (from Ti metal to TiO_2 insulator) enables one to study the effect of scattering atom charges on the calculated XAFS. To calculate XAFS the spherical-wave formalism proposed in [13, 14] is used.

The paper is organized as follows. In section 2 the crystalline potentials and K XAFS of Ti atoms in crystals of Ti, TiC and TiN with metallic conductivity are treated. In section 3 an approximate method of determination of atomic electron configurations used for the phase-shift calculations is proposed. Ti K XAFS of TiO_2 rutile is considered. In section 4 the theoretical Ti metal K XAFS calculated with the help of the generated MT potential using HF, DH and HL potentials for the photoelectron are compared. Section 5 contains a summary and conclusions.

2. Crystalline potentials and Ti K XAFS of crystals of Ti, TiN and TiC

The experimental Ti K XAFS spectra of crystals of Ti, TiC and TiN were presented in [15, 16]. In these papers the experimental spectra were compared with theoretical

ones calculated through the linearized augmented plane-wave (APW) method [17]. The calculated spectra appeared to be contracted on the energy scale. EXAFS analysis of TiN and TiC spectra carried out with the scattering phase shifts and amplitudes proposed in [18] gave essential disagreement in the positions of nitrogen and carbon shells. Balzarotti *et al* [15] concluded that this disagreement is caused by the unsuitable approximation used in [18] for low-Z atom phase-shift calculations.

In order to calculate Ti K XAFS we use in this paper the method described in [14, 19, 20] which takes into account the curvature of photoelectron waves and single, double and triple scattering of the photoelectrons from the surrounding atoms. The crystalline potential is generated according to the rules proposed in [12]. In agreement with the results of [3, 8, 12] we employ an overlapped MT sphere model and set the ionized Ti atom MT sphere radius R_{MT}^{Ti} at 3.25 au so as to provide ~60–70% overlap of the neighbouring MT spheres. As the crystals treated exhibit good metallic conductivity self-consistent HF atomic potentials are calculated for neutral-atom electronic configurations: (i) for ionized Ti atom, $Ti(1s^1 2s^2 \ldots 3d^3 4s^2)$ with d-electron number increased by one to take into account the extra-atomic screening of 1s hole; and (ii) for the surrounding atoms, $Ti(1s^2 2s^2 \ldots 3d^2 4s^2)$, $C(1s^2 2s^2 2p^2)$ and $N(1s^2 2s^2 2p^3)$. The validity of the neutral-atom approximation used in this paper is additionally discussed in section 3.

According to [12] we have to choose MT zero so as to exclude the potential discontinuity Δ at MT sphere surfaces, where $-\Delta$ is the free-atom potential at R_{MT} ($\Delta > 0$). Such an unphysical discontinuity is known to cause artificial electron backscattering oscillations, which distort the x-ray absorption spectra (XAS) fine structure in the energy region of a few tens eV above the threshold [12]. Within the potential model proposed, we neglect the energy dependence of the parameter Δ in this energy region and find $-\Delta$ through summation over the atomic Coulomb and exchange potentials at the chosen R_{MT}^{Ti}, according to the procedure described in [12]. We obtained in such a way Δ = 5.5 eV. The radii of the MT spheres of the surrounding atoms should be chosen so as to exclude also the potential discontinuities at their MT surfaces. The radii R_{MT}^{i} determined under this condition are: $R_{MT}^{Ti} = 3.25$ au, $R_{M,T}^{C} = 2.36$ au, $R_{MT}^{N} = 2.23$ au. Then choosing the MT zero to be shifted by Δ below the free-atom VL, potential continuity at all MT sphere surfaces is achieved.

Using Slater's average energy approximation to calculate exchange potentials inside all atomic spheres we solve radial HF equations for the partial photoelectron wavefunctions $\varphi_l(r)$ in these spheres and obtain as a result HF logarithmic derivatives $L_l^{HF}(\varepsilon) = [\varphi_l^{-1}\, d\varphi_l/dr]_{r=R_{MT}^{i}}$ at MT sphere surfaces, where l is the angular momentum and ε (Ryd) is the photoelectron energy stated from MT zero. Using $L_l^{HF}(\varepsilon)$ the photoelectron scattering phase shifts are calculated for each MT sphere as functions of the photoelectron energy ε and for the angular momenta values $l = 0, 1, \ldots, l_{max}$. The value l_{max} is evaluated by the condition $l_{max} \simeq \sqrt{\varepsilon}\, R_{MT}^{i}$. In the short-wave EXAFS region the maximum value of l appears to be about 20.

The calculated spectra should be compared with experimental ones on the photon energy scale E_{ph}. To carry out such a comparison one needs to combine VL of the crystalline potential with VL position (E_{VL}) in the experimental spectrum. In order to determine E_{VL} on the E_{ph} scale in the case of crystals with metallic conductivity, the following formula is used (see figure 1(*a*)):

$$E_{VL} = E_b + W \tag{1}$$

where E_b is the binding energy of the 1s level determined by x-ray photoelectron spectroscopy (XPS) relative to the Fermi level (E_F) and W is the work function. The

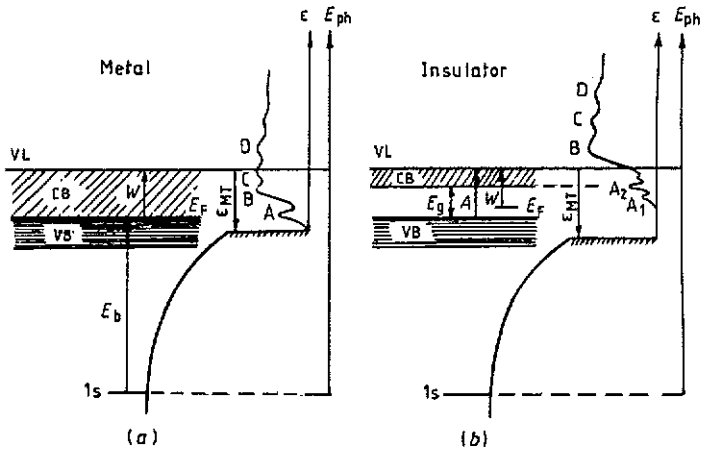

Figure 1. Scheme of the comparison of theoretical and experimental XAFS on the photon energy scale: (*a*) crystals with metallic conductivity; (*b*) insulators.

accuracy of E_b determination does not exceed ~1 eV. Therefore we neglect the small ($\leqslant$1 eV) dependence of W upon the crystal surface choice and use the averaged W values taken from [21].

The theoretical value of the photon energy E corresponding to the photoelectron energy ε started from the MT zero is calculated through the formula:

$$E = \varepsilon + E_b + W - \varepsilon_{MT}$$

where ε_{MT} is the crystalline potential VL position relative to the MT zero.

If one neglects the electron polarization which arises due to the influence of the 1s hole upon the atoms surrounding the ionized one, then the crystalline potential VL coincides with the VL of free atoms and so $\varepsilon_{MT} = \Delta$. However such polarization causes the appearance of a negative Coulomb correction (ε_C) to the crystalline potential in the vicinity of the ionized atom. We consider this correction to be approximately constant and obtain:

$$\varepsilon_{MT} = \Delta + \varepsilon_C. \tag{2}$$

In the molecules and complexes the value ε_C was shown to be about ~5–6 eV [12]. In this paper the same ε_C value is assumed for the insulators and a smaller one ~2–3 eV for the crystals with metallic conductivity.

The extrinsic photoelectron inelastic losses in the present paper are included through the traditional damping factor $\exp[-2R_j/\Lambda(\varepsilon)]$ [1], where R_j is the radius of the jth shell and $\Lambda(\varepsilon)$ is the photoelectron mean free path taken from [17]. The intrinsic losses are included through factor S_0^2, which is taken to be $S_0^2 = 0.8$ for all crystals studied. The number (j_{max}) of shells taken into account is chosen under the rough condition: $2R_{j_{max}} \leqslant \Lambda(\varepsilon_{max})$, where $2R_{j_{max}}$ is the largest single-scattering (SS) photoelectron pathway in the cluster and ε_{max} is the upper energy bound of the calculated spectrum. The atomic thermal vibrations are described through the Debye–Waller factor $\exp(-2\sigma^2k^2)$ [1], where $k^2 = \varepsilon$.

Ti K XAFS calculations of Ti metal, TiC and TiN are performed for energies ε = 10–500 eV above the MT zero. To calculate both near-edge (XANES) and extended absorption

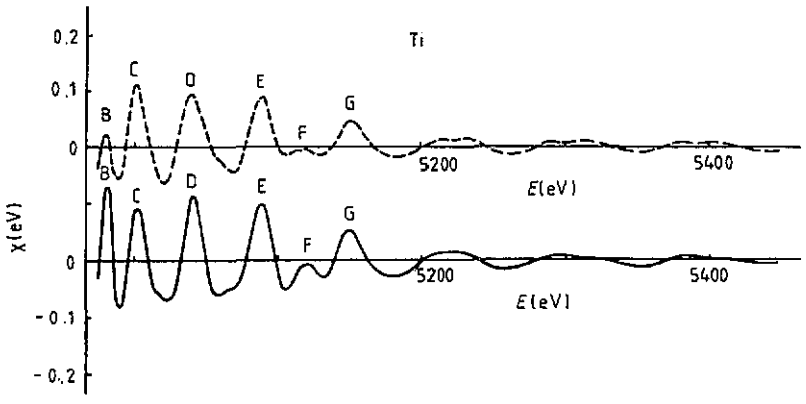

Figure 2. Ti K XAFS function $\chi(E)$ of Ti metal: broken curve, experimental data; full curve, calculated function.

fine structures (EXAFS) we include besides all SS processes [19] in the clusters studied also photoelectron double and triple scattering from the collinear and approximately collinear atomic chains originating at the ionized Ti atoms [20]. Such approximation is known to give theoretical XANES in reasonable agreement with experimental ones for many crystals [20, 22].

2.1. Ti K XAFS of Ti metal

Metallic titanium is a crystal with HCP structure [23] with the nearest to the ionized Ti atom shell radii: $R_1 = 5.5$ au, $R_2 = 5.57$ au, $R_3 = 7.83$ au. For Ti metal the value $\Lambda(\varepsilon)$ increases from ~12 au at $\varepsilon \sim 30$ eV to 25 au at $\varepsilon \sim 500$ eV [17]. Therefore a Ti cluster with outer shell radius 12.43 au was chosen. The photoelectron SS processes and the focusing processes for the eighth-shell atoms 'shadowed' by the second-shell atoms are taken into account for XANES and EXAFS calculations. In the following a simplified notation for such approximation is used:

$$\text{SS} + 6[\text{Ti(ionized atom)} - \text{Ti(2nd shell)} - \text{Ti(8th shell)}]$$

where the coefficient 6 denotes the number of identical atomic chains. In figure 2 the theoretical EXAFS function $\chi^{\text{th}}(E)$ is compared with the experimental one $\chi^{\text{exp}}(E)$ [15] by combining VL positions at both spectra as was described earlier. The value $E_{\text{VL}}^{\text{exp}}$ is calculated by the formula (1) through the summation of 1s binding energy $E_b = 4965$ eV [24] and $W = 4$ eV [21] in Ti metal, which gives $E_{\text{VL}}^{\text{exp}} = 4969$ eV.

In figure 3 the theoretical Ti K photoionization cross section $\sigma^{\text{th}}(E)$ in the near-edge region is compared with the experimental cross section $\sigma^{\text{exp}}(E)$. The calculation is carried out through the formula [19]:

$$\sigma^{\text{th}}(E) = \sigma_0^{\text{th}}(E)[1 + \chi(E)]$$

where $\sigma_0^{\text{th}}(E) \sim |\langle \varphi_{\varepsilon p} | \nabla | \varphi_{1s} \rangle|^2$ is the free atomic sphere K photoionization cross section, φ_{1s} is the wavefunction of the 1s level and $\varphi_{\varepsilon p}$ is the single-particle wavefunction of the final photoelectron state of p symmetry at energy ε.

As one can see from figures 2 and 3 the crystalline potential model employed in this paper enables one to obtain not only EXAFS but also the main peaks B and C of XANES

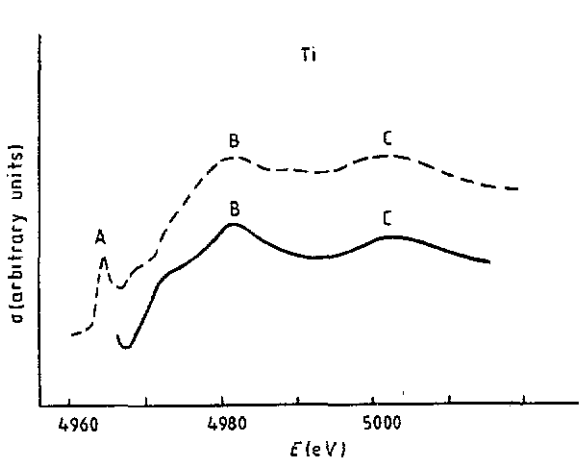

Figure 3. Ti K absorption cross section $\sigma(E)$ of Ti metal on an expanded energy scale: broken curve, experimental data; full curve, calculated function.

in good agreement with experiment. The absence of some details of K photoionization cross section in the near-edge region could be explained by the influence of those photoelectron multiple scattering (MS) processes which have not been taken into account in our calculations.

2.2. Ti K XAFS of TiC and TiN crystals

TiC and TiN are crystals with the rock-salt structure [23]. The values $\Lambda(\varepsilon)$, S_0^2 and σ^2 are chosen to be the same as for Ti metal. XAFS calculations are carried out with the help of clusters which contain the ionized Ti atom surrounded by seven neighbouring shells. There are two types of collinear atomic chains in these clusters: (i) the fourth-shell atoms are 'shadowed' by the first-shell atoms; (ii) the seventh-shell atoms are 'shadowed' by the second-shell ones. The inclusion of photoelectron multiple scattering (focusing processes) from these chains is crucial to obtain agreement with experiment. Therefore in EXAFS region the following scattering processes should be taken into account:

$$\text{ss} + 6[\text{Ti(ionized atom)} - \text{C or N(1st shell)} - \text{Ti(4th shell)}]$$
$$+ 12[\text{Ti(ionized atom)} - \text{Ti(2nd shell)} - \text{Ti(7th shell)}].$$

Ti K EXAFS of TiN and TiC crystals appear to be in good agreement with experiment [15] in the energy region $\varepsilon \geqslant 150$ eV above the MT zero. However in the energy region $\varepsilon \leqslant 150$ eV some discrepancies of the peak relative intensities compared with the experimental ones occur. Therefore, in this region we use the results of [20] concerning XAFS formation in crystals with the rock-salt structure. According to [20] in order to achieve agreement with experiment in the low-energy region one should take into account photoelectron MS processes in approximately collinear atomic chains

$$\text{Ti(ionized atom)} - \text{C or N(1st shell)} - \text{Ti(2nd shell)}$$

chosen under the empirically obtained 'selection rules'. Such a MS contribution to $\chi(\varepsilon)$ falls with increasing photoelectron energy, but in the energy region $\varepsilon \leqslant 150$ eV it gives

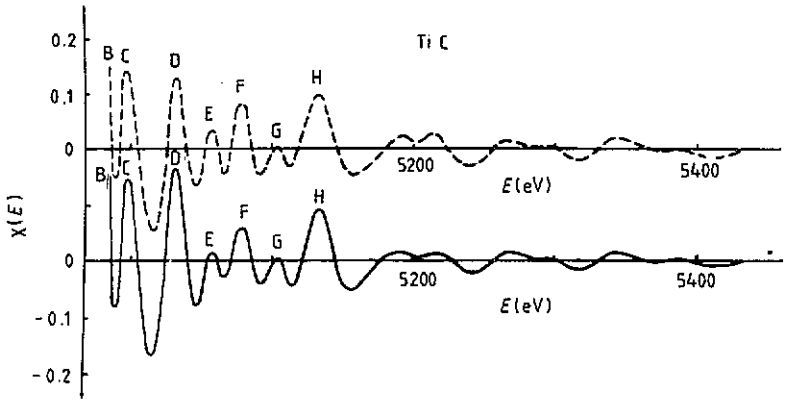

Figure 4. Ti K XAFS function $\chi(E)$ of TiC: broken curve, experimental data; full curve, calculated function.

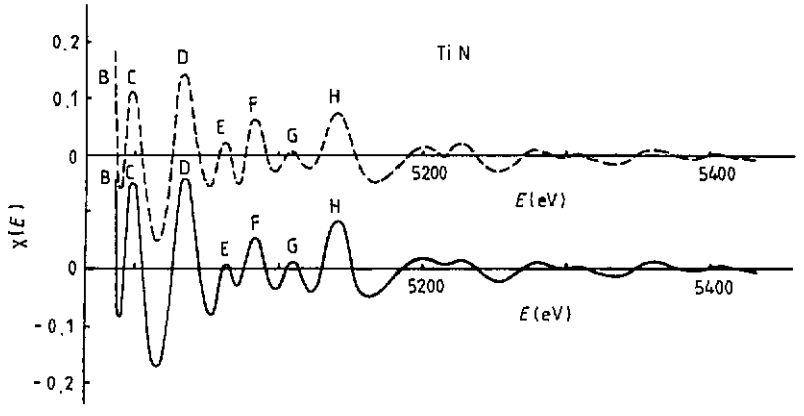

Figure 5. Ti K XAFS function $\chi(E)$ of TiN: broken curve, experimental data; full curve, calculated function.

the opportunity to obtain theoretical XAFS in agreement with the experimental one and to determine the renormalized backscattering amplitude for the second-shell atoms [25] . To compare theoretical and experimental XAFS on the E_{ph} scale, VL positions in the experimental spectra are calculated through formula (1): for TiC, E_{VL}^{exp} = 4965.4 eV [24] + 2.6 eV [21] = 4968.0 eV; and for TiN, E_{VL}^{exp} = 4966.5 eV [24] + 2.9 eV [21] = 4969.4 eV. As one can see from figures 4 and 5 the comparison of $\chi^{th}(E)$ with $\chi^{exp}(E)$ shows their good overall agreement on the E_{ph} scale. In the near-edge region the theoretical Ti K photoionization cross section $\sigma^{th}(E)$ of TiN crystal is compared in figure 6 with the experimental one $\sigma^{exp}(E)$. The same comparison for TiC crystal appears to be quite similar and therefore is not presented. So the approximation used gives the main peaks B and C of Ti K XANES in good agreement with the experiment on the E_{ph} scale for all crystals with metallic conductivity (Ti metal, TiN and TiC).

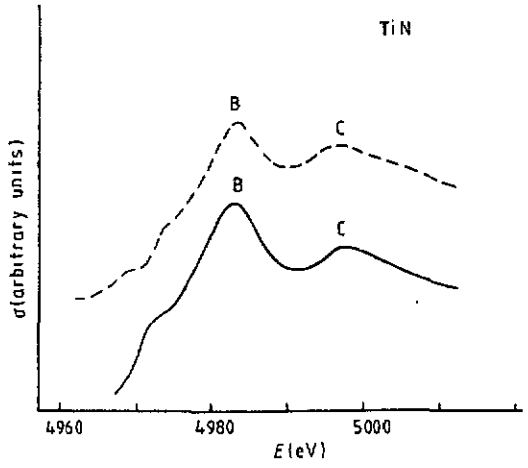

Figure 6. Ti K absorption cross section $\sigma(E)$ of TiN on an expanded energy scale: broken curve, experimental data; full curve, calculated function.

3. Crystalline potential and Ti K XAFS of TiO_2 rutile

The results obtained in [5, 6, 8, 12, 26] and in section 2 of this paper show that the MT potential model that employs the free neutral-atom potentials inside MT spheres is good enough for covalent binding and metallic systems. It is not obvious, however, whether this model would provide good results for ionic crystals. We treat this problem below using as an example Ti K XAFS of TiO_2 rutile. First we show how one could get information about electronic configurations of the atoms in solids by exploiting x-ray absorption spectra.

3.1. Choice of atomic electron configuration for phase-shift calculations in solids

In this section an approximate method of electronic configuration determination for the purpose of phase-shift calculations is proposed. The method is based on the direct comparison of the experimental K absorption threshold energy (E_K^{exp}) with the theoretical one (E_K^{th}). As an example the method proposed is used to determine appropriate electronic configurations of Cu, Fe and Ti atoms in metals. If the initial configuration of an Fe atom in the crystal is $Fe(1s^2 \ldots 3d^6 4s^2)$ then to obtain $E_K^{th}(Fe)$ the final configuration $Fe(1s^1 2s^2 \ldots 3d^7 4s^1 4p^1)$ should be used in which the 1s electron is excited to the first unfilled level of p symmetry and one of the 4s electrons transfers to the 3d level to simulate extra-atomic screening of the 1s hole. The theoretical K threshold energy could be calculated approximately by subtracting from the total energy of the final atomic state that of the initial state. We have carried out the total energy calculations with the help of a non-relativistic HF program without taking into account the correlation effects. Therefore the relativistic (d^{rel}) and correlation (d^{corr}) corrections should be added to HF energy E_K^{HF}, i.e.

$$E_K^{th} = E_K^{HF} + d^{rel} + d^{corr} = E_K^{HF} + d.$$

To evaluate the total corrections d for Cu, Fe and Ti atoms we have calculated these corrections for Ar, Kr and Xe atoms as the differences between the experimental K

threshold energies [27] and those obtained through HF calculations [28]. The values obtained appear to depend upon atomic number as $Z^{4.39}$. Using $Z^{4.39}$ interpolation over Ar, Kr and Xe data we have found the following results: $d_{Cu} = 86.9$ eV, $d_{Fe} = 53.8$ eV and $d_{Ti} = 25.8$ eV. Then for the proposed configurations of the initial and final states of the Fe atom one obtains the theoretical threshold energy $E_K^{th}(Fe) = 7110.7$ eV, in good agreement with the experimental one, $E_K^{exp}(Fe) = 7111.0$ eV [16]. This result justifies the validity of the configuration $Fe(1s^2 \ldots 3d^64s^2)$ to calculate phase shifts for the surrounding Fe atoms and $Fe(1s^12s^2 \ldots 3d^74s^2)$ to calculate the p phase shift for the ionized atom. Similar analysis carried out for Cu and Ti crystals for the initial state configurations $Cu(1s^2 \ldots 3d^{10}4s^1)$ and $Ti(1s^2 \ldots 3d^24s^2)$ gives $E_K^{th}(Cu) = 8980.5$ eV ($E_K^{exp}(Cu) = 8980.0$ eV [16]) and $E_K^{th}(Ti) = 4968$ eV ($E_K^{exp} = 4965$ eV [16]). As before, comparison with experiment justifies the validity of the configurations $Cu(1s^2 \ldots 3d^{10}4s^1)$ and $Ti(1s^2 \ldots 3d^24s^2)$ for the phase-shift calculations for the surrounding atoms and $Cu(1s^12s^2 \ldots 3d^{10}4s^2)$ and $Ti(1s^12s^2 \ldots 3d^34s^2)$ for p phase-shift calculations for the ionized atoms in metallic Cu and Ti crystals.

The variation of sp-electron number by one causes approximately ~3–5 eV shifts of E_K^{th} for all d elements, while the variation of d-electron number causes a shift that increases from ~5 eV for light transition atoms to ~15 eV when the 3d shell is filled. This result enables one to determine the valence electron distibution between 3d and sp states through comparison of the values E_K^{th} and E_K^{exp}.

3.2. Ti K XAFS of TiO_2 rutile

TiO_2 rutile is an insulator with energy gap $E_g \sim 3$ eV and experimental Ti K absorption threshold energy $E_K^{exp}(Ti) = 4971.8$ eV [16]. The theoretical threshold energy $E_K^{th}(Ti)$ calculated as proposed in section 3.1 using the electronic configurations $Ti^+(1s^2 \ldots 3d^24s^1)$ for the initial state and $Ti^+(1s^12s^2 \ldots 3d^34p^1)$ for the final state of the ionized Ti atom appears to be equal to 4971 eV, which is much closer to $E_K^{exp}(Ti)$ than that obtained within the neutral-atoms (NA) model. Therefore the ionic model (ION model) for TiO_2 crystal based on Ti^+ and $O^{0.5-}$ free-ion potentials is preferable for the scattering phase-shift and amplitude calculations. Unfortunately, such a model provides non-transferable scattering phase shifts and amplitudes, which causes XAFS analysis limitations. It was shown in [10, 11] that sometimes both NA and ION models give similar near-edge XAFS. Taking this result into account we calculate Ti K XAFS of TiO_2 rutile in this section using the NA model.

The nearest-shell radii in TiO_2 rutile according to [23] are $R_1 = 3.56$ au, $R_2 = 3.72$ au and $R_3 = 5.46$ au. The values $\Lambda(\varepsilon)$, S_0^2 and σ^2 are assumed to be the same as for Ti metal, TiC and TiN. The ε_{MT} value is obtained by formula (2) using the values $\Delta = 5.5$ eV and $\varepsilon_C = 6$ eV. A cluster with outer Ti shell radius 10.15 au is employed. The SS approximation added with the contributions from electron focusing processes in the collinear atomic chains Ti(ionized atom) – O(2nd shell) – O(8th shell) is used to calculate Ti K XAFS of TiO_2. As before the comparison of the theoretical and experimental spectra is performed by combining their VL positions. However, the problem of E_b determination in insulators with the help of XPS data is rather difficult; hence to determine VL position in the experimental Ti K XAFS of TiO_2 an alternative approach is employed. Its idea is schematically illustrated in figure 1(*b*). The basis is that the peak A_2, which occurs in every cation K absorption spectra of transition-metal oxides studied in [16, 29], is caused by 1s electron excitation to the first unfilled hybridized pd state [16] and within an

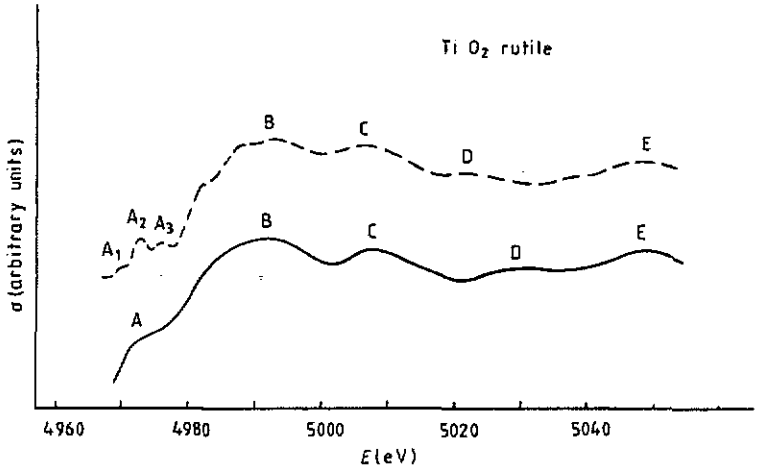

Figure 7. Ti K absorption cross section $\sigma(E)$ of TiO_2 rutile on an expanded energy scale: broken curve, experimental data; full curve, calculated function.

accuracy of ~1–1.5 eV this peak determines the position of the conduction band bottom (E_{CB}) on the E_{ph} scale. Then one obtains

$$E_{VL}^{exp} = E_{CB} + A - E_g \tag{3}$$

where A is the photocurrent threshold.

Taking into account that A slightly exceeds ($\leq$1–1.5 eV) W, we use approximately $A \simeq W$. In the case of TiO_2 rutile $W = 3.8$ eV [21] and $E_{CB} = 4971.8$ eV [29]. The formula (3) gives $E_{VL}^{exp} = 4972.6$ eV. In figure 7 the theoretical Ti K photoionization cross section $\sigma^{th}(E)$ is compared with the experimental one $\sigma^{exp}(E)$. One could see that the calculated positions and relative intensities of the main peaks B, C and E in the theoretical spectrum are in reasonable agreement with those of the experimental spectrum. Of course, if one would like to reach better agreement of the theoretical and experimental spectra in the low-energy region $\varepsilon \leq 20$ eV as well as in peak D energy position, other MS processes should be involved. We see that the NA model enables one to calculate XAFS in reasonable agreement with experiment. The theoretical Ti K XAFS function $\chi(E)$ of TiO_2 rutile is shown in figure 8 for energies ε = 10–500 eV above the MT zero.

4. DH exchange and HL exchange–correlation potentials in the Ti K XAFS calculations

The DH exchange potential is known to give the best approximation to HF phase shifts and amplitudes of covalent binding and metallic systems in EXAFS energy region [8, 12]. We now present the results of Ti metal K XAFS calculations carried out by the crystalline MT potential proposed in section 2, and the only change made consists of the replacement of the HF interaction for the photoelectrons inside MT spheres by the DH one. Ti XAFS function $\chi_{DH}(E)$ calculated with the help of this potential is compared in figure 9 with the function $\chi_{HF}(E)$ obtained in section 2.

To examine the adequacy of HL exchange–correlation potential for XAFS analysis, Ti metal K XAFS has been calculated with the help of the MT potential obtained by the

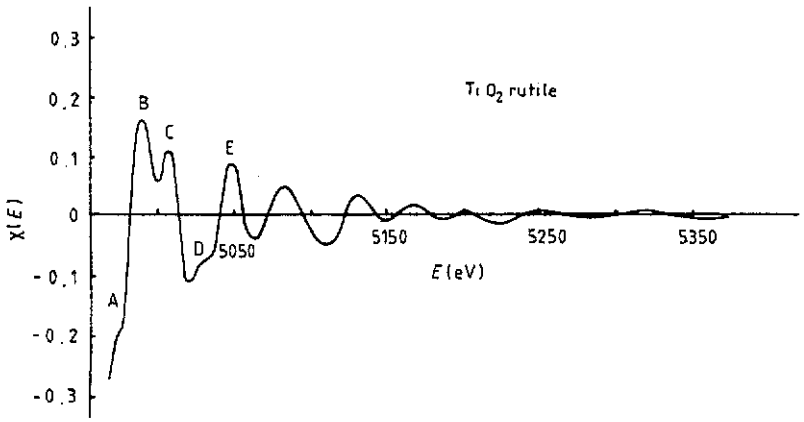

Figure 8. Theoretical Ti K XAFS function $\chi(E)$ of TiO_2 rutile over an extended energy range.

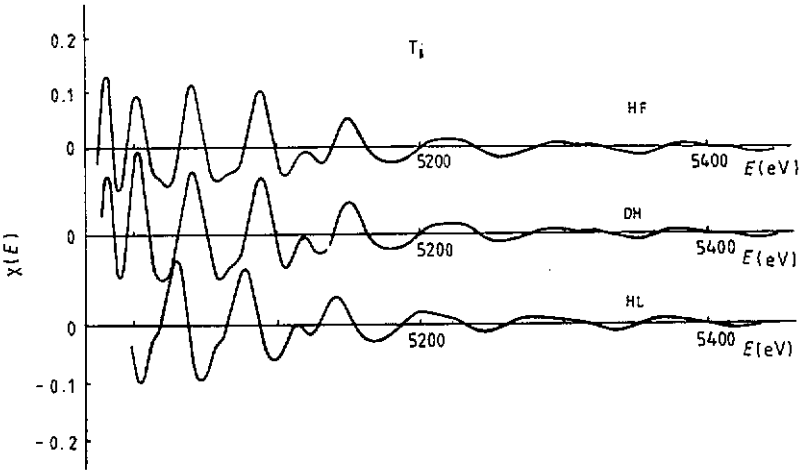

Figure 9. Theoretical Ti K XAFS function $\chi(E)$ of Ti metal calculated through MT potential with various forms of exchange–correlation interaction of the photoelectrons with core electrons inside MT spheres.

replacement of the HF interaction for the photoelectrons inside MT spheres by the HL one. To simplify the calculations we have used the assumption made in [3] that the imaginary part of the HL potential is much smaller than its real part (Re(HL)). Besides, the approximate analytical expression for Re(HL) given in expression (3.10a) of [3] has been employed. Using the Re(HL) potential inside MT spheres instead of the HF one, the scattering phase shifts and amplitudes have been calculated. We have found that the replacement of the HF potential by the HL one inside MT spheres without change of ε_{MT} causes a small potential discontinuity of the crystalline potential at MT sphere surfaces in the near-edge region $\varepsilon \leqslant 100$ eV. As far as the analytical expression (3.10a) of [3] is appropriate in the range $k = 2$–10 au, Ti metal K XAFS function $\chi_{HL}(E)$ has been calculated only for the energy region $\varepsilon = 55$–500 eV above the MT zero. The calculated

XAFS functions $\chi_{HF}(E)$, $\chi_{DH}(E)$ and $\chi_{HL}(E)$ are shown in figure 9. One can see that functions $\chi_{HF}(E)$ and $\chi_{DH}(E)$ are in good overall agreement both in relative peak intensities and in their positions on the photon energy scale. These functions agree with good accuracy with the experimental one. The agreement of the function $\chi_{HL}(E)$ with experiment in relative positions and intensities of the peaks is slightly worse. Moreover, the function $\chi_{HL}(E)$ is shifted by more than 10 eV on the photon energy scale relative to the experimental function $\chi(E)$. Hence one should presume that the HL exchange–correlation potential for the photoelectrons inside MT spheres is inappropriate if the MT potential model proposed in [12] and in this paper is employed.

5. Summary and conclusions

We have presented a method of crystalline MT potential generation that employs HF interaction between the photoelectron and core electrons inside MT spheres. Theoretical Ti K XAFS of Ti metal, TiC, TiN and TiO_2 rutile crystals are calculated using the potential model proposed and the spherical-wave formalism to describe electron scattering processes. We have achieved overall agreement of the theoretical and experimental spectra on the photon energy scale within an accuracy of ~2–3 eV. This small discrepancy may be due to several reasons: inaccuracy of VL determination in the experimental spectra; non-muffin-tin effects not taken into account; electron charge transfer which is neglected in terms of the neutral-atoms model used; electron correlation effects; and so on. Nevertheless the accuracy obtained is sufficient to justify the adequacy of the proposed MT potential model for phase-shift calculations, and the model proposed could enable one to determine the absorber environment atom type by XAFS. The basis is that the absolute values of scattering phase shifts are more sensitive to atomic number variations than their derivatives. In [30] a new method of environment atom type determination was proposed which was based on the comparison of the theoretical and experimental values of the backscattering amplitude phases. It is evident that, to carry out such a comparison, one needs to determine the MT zero position of the crystalline potential relative to the VL position on the experimental spectrum without any fitting procedure and to have precise absolute values of theoretical phase shifts and scattering amplitudes on the E_{ph} scale.

The results of the present paper together with the results of [12] may be summarized as the following rules of MT potential generation and scattering phase-shift and amplitude calculations:

(i) The MT sphere of each atom should be overlapped with the neighbouring spheres as much as possible; however, the strong potential regions of the neighbouring atoms must not be included.

(ii) HF or DH exchange interaction between the photoelectrons and core electrons inside MT spheres and the spherical-wave formalism should be used for photoelectron scattering phase-shift and amplitude calculations. To obtain the more distant shadowed shells contributions to XAFS, the electron focusing processes in collinear atomic chains should be taken into account.

(iii) To calculate the phase shifts for the absorbing atom one needs to use the electronic configuration with a core hole at the ionized level and the valence electron number increased by one because of the extra-atomic screening processes. The neutral-atom potentials are employed for the surrounding atoms.

(iv) MT sphere radii R_{MT} should be chosen so as to make the potential discontinuity values at these radii equal for all MT spheres. The MT zero position should be chosen then to provide potential continuity at every MT sphere surface. The MT zero position determined with respect to the crystalline or molecular VL is obtained through summation over the potential discontinuity value (Δ) at R_{MT} determined relative to the free-atom VL and the Coulomb correction (ε_C) which arises due to the polarization of the environment atoms caused by the 1s hole at the absorbing atom.

(v) The criterion of the adequacy of the generated MT potential is the agreement of theoretical and experimental XAFS on the photon energy scale.

References

[1] Koningsberger D C and Prins R 1988 *X-Ray Absorption: Principles, Applications, Techniques of EXAFS, SEXAFS and XANES* (New York: Wiley) p 670
[2] Lee P A and Beni G 1977 *Phys. Rev.* B **15** 2862–83
[3] Chou S H, Rehr J J and Stern E A 1987 *Phys. Rev.* B **35** 2604–14
[4] Dan Lu, Mustre de Leon J and Rehr J J 1989 *Physica* B **158** 413–4
[5] Rehr J J, Mustre de Leon J, Zabinsky S I and Albers R C 1990 *Preprint* University of Washington, Seattle, p 20
[6] Sainctavit Ph, Petiau J, Benfatto M and Natoli C R 1989 *Physica* B **158** 347–50
[7] Vedrinskii R V, Bugaev L A, Gegusin I I, Kraizman V L, Novakovich A A, Prosandeev S A, Ruus R E, Maiste A A and Elango M A 1982 *Solid State Commun.* **44** 1401–7
[8] Vedrinskii R V, Bugaev L A and Levin I G 1989 *Physica* B **158** 421–4
[9] Vedrinskii R V, Bugaev L A and Levin I G 1988 *Opt. Spectrosk.* **65** 537–9
[10] Bugaev L A, Gegusin I I, Datsyuk V N, Novakovich A A and Vedrinskii R V 1986 *Phys. Status Solidi* b **133** 195–202
[11] Gegusin I I, Datsyuk V N, Novakovich A A, Bugaev L A and Vedrinskii R V 1986 *Phys. Status Solidi* b **134** 641–50
[12] Vedrinskii R V, Bugaev L A and Airapetian V M 1991 *J. Phys. B: At. Mol. Opt. Phys.* **24** 1967–75
[13] Vedrinskii R V and Bugaev L A 1986 *J. Physique Coll.* vol C8 89–92
[14] Bugaev L A, Vedrinskii R V and Levin I G 1989 *Physica* B **158** 378–82
[15] Balzarotti A, De Crescenzi M and Incoccia L 1982 *Phys. Rev.* B **25** 6349–65
[16] Grunes L A 1983 *Phys. Rev.* B **27** 2111–31
[17] Muller J E, Jepsen O and Wilkins J W 1982 *Solid State Commun.* **42** 365–8
[18] Teo B K and Lee P A 1979 *J. Am. Chem. Soc.* **101** 2815–32
[19] Bugaev L A and Vedrinskii R V 1985 *Phys. Status Solidi* b **13** 459–64
[20] Vedrinskii R V, Bugaev L A and Levin I G 1988 *Phys. Status Solidi* b **150** 307–14
[21] Riviere J C 1969 *Solid State Surface Science* ed M Green (New York: Dekker) p 432
[22] Bianconi A, Garcia J and Benfatto M 1988 *Topics Current Chem.* **145** 30–67
[23] Landolt-Börnstein 1955 *Zahlenwerte und Funktionen Aus. Kristalle* (Berlin: Springer) p 1007
[24] Wagner C D 1983 *Practical Surface Analysis by Auger and X-Ray Photoelectron Spectroscopy* ed D Briggs and M P Seach (New York: Wiley) p 598
[25] Bugaev L A, Vedrinskii R V and Permjakov S V 1991 *Proc. 6th Int. Conf. on X-Ray Absorption Fine Structure (York)* ed S S Hasnain (New York: Ellis Horwood) pp 72–4
[26] Norman D, Garg K B and Durham P J 1985 *Solid State Commun.* **56** 895–8
[27] Siegbahn K, Nordling C, Fahlman A, Nordberg R, Hamrin K, Hedman J, Johansson G, Bergmark T, Karlsson S-E, Lindgren I and Lindberg B 1967 *ESCA (Atomic, Molecular and Solid State Structure Studied by Means of Electron Spectroscopy) (Uppsala)* p 493
[28] Kuchas S A, Karasene A V and Karazia R I 1978 *Litovskii Fiz. Sbornik* **18** 593–601
[29] Balzarotti A, Comin F, Incoccia L, Piacentini M, Mobilio S and Savoia A 1985 *Solid State Commun.* **35** 145–9
[30] Halaka F G, Boland J J and Baldeschwieler J D 1984 *J. Am. Chem. Soc.* **106** 5408–13